 https://doi.org/10.69107/jid-157414

Published Online: 2024 December 31

Research Article

Dose Changes Caused by Placing a Surgical Mask Inside the Radiotherapy Treatment Field

Azam Janati Esfahani [1,2,*], Leila Azimi [3], Mohammadreza Saghafi [3]

[1] Cellular and Molecular Research Center, Research Institute for Prevention of Non-communicable Disease, Qazvin University of Medical Sciences, Qazvin, Iran

[2] Department of Medical Biotechnology, School of Advanced Technologies in Medicine, Qazvin University of Medical Sciences, Qazvin, Iran

[3] Clinical Research Development Unit, Velayat Hospital, Qazvin University of Medical Sciences, Qazvin, Iran

[*] ***Corresponding Author:*** Cellular and Molecular Research Center, Research Institute for Prevention of Non-communicable Disease, Qazvin University of Medical Sciences, Qazvin, Iran. Email: janaty.azam@gmail.com

Received: 20 October, 2024; **Revised:** 30 November, 2024; **Accepted:** 22 December, 2024

Abstract

Background: The present study investigated the effect of the presence of medical masks in or near the radiotherapy (RT) treatment field during the COVID-19 pandemic, due to the widespread use of medical masks on the faces of patients undergoing RT.

Methods: The dose distribution was calculated in a polymethyl methacrylate (PMMA) phantom using the Monaco treatment planning system, and then measured in a water phantom beneath the surgical medical mask (SMM) and near the mask, for photon energies of 6, 10, and 18 MV, and electron energies of 6, 8, 10, 12, and 15 MeV, emitted from a Versa HD linac.

Results: According to the Monaco results, the difference in dose distribution between the area under the mask and the area outside the mask was observed only up to a depth of 20 mm. In electron radiation, this difference was observed up to a depth of 10 mm. Based on the measurement results, we found that at the entrance plane of the phantom, the masked readings increased by 1.2, 1.18, and 1.14 times compared to the unmasked mode for photon energies of 6, 10, and 18 MV, respectively. The masked readings increased by 3.1%, 3.4%, 3.2%, 2.6%, and 1.3% compared to the unmasked mode for 6, 8, 10, 12, and 15 MeV, respectively.

Conclusions: Medical masks altered the dose distribution of both photon and electron radiation within the main treatment field and outside the main field, particularly at the surface. It is therefore recommended to keep patients' medical masks out of the radiated field.

Keywords: Medical Mask, Photon, Electron, Radiation Dose, COVID-19

1. Background

The COVID-19 pandemic significantly impacted various aspects of healthcare, including radiotherapy (RT) (1, 2). Studies have shown that individuals with active cancer are at a higher risk of death from COVID-19 compared to the general population (20% vs. 1.8 - 7.2%) (3-6). A medical mask-wearing policy for patients undergoing RT was implemented at the beginning of the COVID-19 pandemic and continues for some patients due to the emergence of new respiratory viruses caused by mutations in coronaviruses and types of influenza that may still be present in the environment (7-9). In some medical centers, wearing two or more layers of medical masks has been recommended for enhanced protection (10). Surgical medical masks (SMMs) typically have a tri-layered structure, including a thin metallic strip to secure the mask over the nose. The middle layer functions as a filter, while the inner layer absorbs moisture, and the outer layer repels water (11).

The presence of a medical mask during RT treatments may pose unique challenges in terms of dosimetry. Dosimetry is a critical aspect of RT, aiming to accurately calculate and deliver radiation doses to cancer patients while minimizing the impact on healthy tissues (12). Similar to patient gowns or thermoplastic devices used in RT, the use of a face mask during

How to Cite: Janati Esfahani A, Azimi L, Saghafi M. Dose Changes Caused by Placing a Surgical Mask Inside the Radiotherapy Treatment Field. J Inflamm Dis. 2024; 28 (4): e157414. https://doi.org/10.69107/jid-157414.

treatment may introduce dosimetry-related issues such as radiation attenuation, backscatter, material heterogeneity, surface contouring, electron interaction, and setup variations (13-15). These devices typically alter the surface dose (16).

The metallic strip of the surgical mask, usually made of aluminum or another malleable material, has a higher probability of absorbing photons and electrons compared to other substances commonly used in surgical masks (17). Consequently, there is a potential for increased localized radiation attenuation in the vicinity of the metal strip, leading to discrepancies in dose distribution.

2. Objectives

Due to the consistent use of medical masks on the faces of patients RT treatment during the COVID-19 pandemic, and given the scarcity of published data regarding dose attenuation caused by medical masks, the presnet study aimed to investigate the effect of placing SMMs inside the treatment field or near the field in terms of changes in radiation dose distribution.

3. Methods

In this study, we investigated the changes in radiation dose distribution caused by the presence of a tri-layered SMM made from polypropylene, using both calculations in the treatment planning system and measurements in a water phantom.

Irradiation was performed using a linear accelerator, the Versa HD™ (Elekta Oncology Systems, Crawley, UK), which delivers three photon beams with nominal energies of 6, 10, and 18 MV, as well as five electron beams with nominal energies of 6, 8, 10, 12, and 15 MeV. Calculations and measurements were carried out for all photon and electron energies.

3.1. Medical Mask Dose Calculation for Electron and Photon Energies

A cubic phantom made of polymethyl methacrylate (PMMA), consisting of 23 slabs each with a thickness of one centimeter and dimensions of 200 × 200 mm, was used in this study. The phantom was positioned on the table of a 16-slice computed tomography (CT) scanner (Siemens, Germany). The CT images were acquired both with and without the presence of three layers of the SMM placed on the phantom (Figure 1). Images were captured with a slice thickness of 3 mm and transferred to the Monaco treatment planning system (Elekta, Monaco 5.11, UK) for target volume delineation and treatment plan design.

The dose distribution was calculated within the phantom using a 100 × 100 mm radiation field for all photon and electron energies. Calculations were carried out from the surface to a depth of 230 mm under two conditions: (A) with SMM (under the mask), and (B) 50 mm adjacent to the SMM (no mask). Dose calculations for photon radiation were performed using the collapse cone dose calculation algorithm, while those for electron beams were conducted using the Monte Carlo algorithm. In this section, the dose enhancement ratio and transmission factor were defined at a depth of 100 mm as follows:

Calculated dose enhancement ratio (CER) = Dose at open field close to the SMM/dose under the SMM

Calculated transmission factor (CTF) = Dose under the SMM/dose at open field

3.2. Medical Mask Dose Measurements at Electron and Photon Radiation

Relative and absolute dosimetry measurements were performed using a BeamScan water phantom (PTW, Freiburg, Germany). A portion of the phantom was covered with a tri-layered SMM, while the remaining part was left uncovered to serve as a control.

By positioning an ion chamber beneath the SMM, it was possible to measure the radiation dose received in the area specifically covered by the SMM material. By comparing measurements taken with and without the SMM, the surface dose enhancement factor was evaluated under constant temperature and pressure conditions using the following relationship:

Measured dose enhancement ratio (MER) = Dosimeter reading with SMM/dosimeter reading without SMM

Additionally, the transmission factor, which represents the attenuation caused by the SMM, was defined as:

Measured transmission factor (MTF) = Dosimeter reading with SMM (d = 100 mm)/dosimeter reading without SMM (d = 100 mm)

3.2.1. Photon Percentage Depth Dose

To investigate the effect of the SMM on radiation dose distribution, relative dosimetry was performed both with and without the presence of the SMM in the

Figure 1. Set up of surgical medical mask (SMM) on polymethyl methacrylate (PMMA) phantom for computed tomography (CT) scan

radiation field. Measurements were conducted once under the mask and once adjacent to the main radiation field.

For relative dosimetry, two Semiflex 3D chambers (PTW, Freiburg, Germany), each with an active volume of 0.125 cc, were used. One chamber was placed in the air at the corner of the field to serve as a reference dosimeter, while the other was used as the measuring dosimeter positioned inside the water phantom within the radiation field. The measuring dosimeter was gradually moved from the surface to a depth of 300 mm in the water, and the electric charge collected for 6, 10, and 18 MV photon radiation was recorded in nanocoulombs (nC) along the central axis of the beam using the MEPHYSTO mc^2 software (PTW, Freiburg, Germany). The readings were normalized to the maximum value and presented as the percentage depth dose (PDD).

The PDD measurements were performed under the following four conditions: (A) Open field, without SMM (no mask); (B) within the field, under the SMM (with mask); (C) outside the field, 50 mm adjacent to the main radiation field, with SMM; (D) outside the field, 50 mm adjacent to the main radiation field, without SMM. Each measurement was compared against its corresponding control group. The use of individual control groups accounted for any uncertainties introduced by setup variations and positional errors.

3.2.2. Electron Percentage Depth Dose

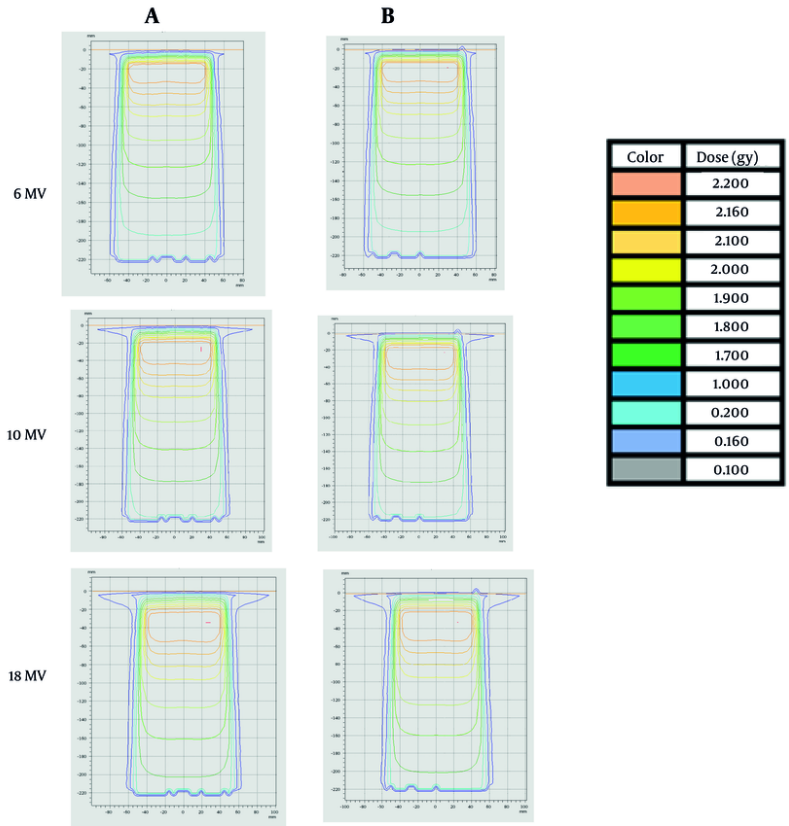

Figure 2. Isodose lines of X-ray radiation in energies of 6, 10 and 18 MV inside the polymethyl methacrylate (PMMA) phantom in a 10 × 10 cm field: A, with surgical medical mask (SMM) (under the mask); B, 5 cm next to the SMM (no mask).

For electron relative dosimetry, similar to the photon dosimetry procedure, a Semiflex 3D dosimeter was used. A 100 × 100 mm electron applicator was employed to measure the amount of collected charge for electron radiation energies of 6, 8, 10, 12, and 15 MeV. The PDD measurements were performed from the water surface to a depth of 80 mm under two conditions: (A) Without SMM (outside the mask), and (B) with SMM (under the mask). Based on the data obtained from the photon depth dose measurements, we were able to determine the percentage difference in dose between the masked and unmasked conditions. The difference percentage was calculated using the following formula: Difference percentage = (Dosimeter readindg under mask - Dosimeter reading in open field) × 100/Dosimeter reading in open field.

4. Results

4.1. TPS Dose Calculation Results

The dose distribution in the form of isodose curves for 6, 10, and 18 MV photon energies is shown in Figure 2 for both conditions (with and without the SMM). The corresponding results for electron energies are illustrated in Figure 3.

Only slight differences were observed between the isodose distributions, which were noticeable up to a depth of 20 mm. The CER and CTF were computed at a depth of 100 mm inside the PMMA phantom. The results are presented in Table 1.

The presence of the SMM in the radiation field led to a reduction in the delivered dose as follows: Approximately 3.5% for 6 MV, 3.1% for 10 MV, and about 0.6% for 18 MV photon energy. This reduction is attributed to scatter caused by the mask material, which

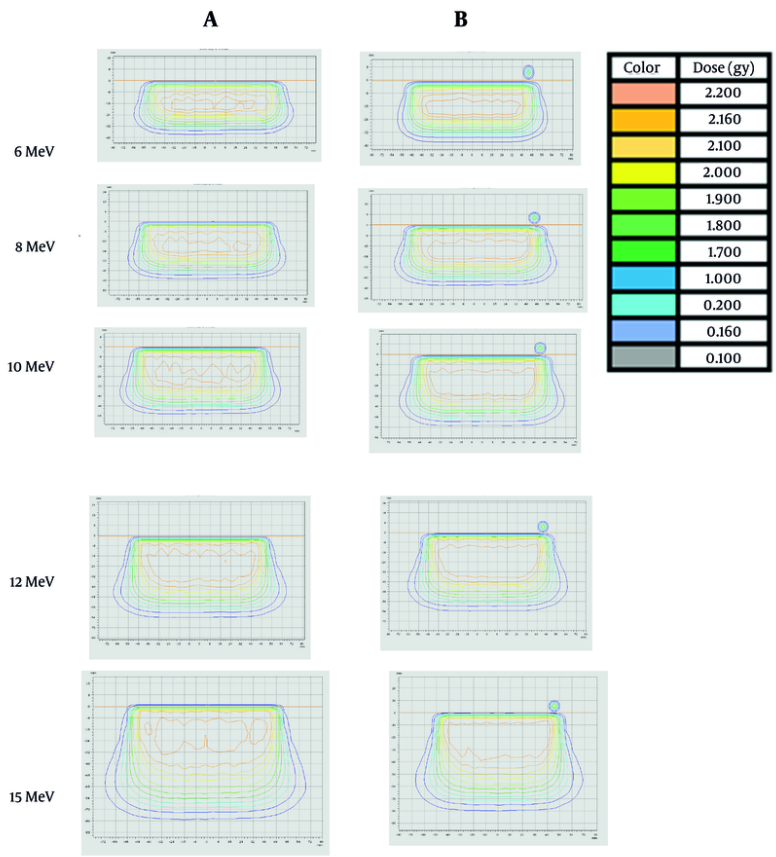

Figure 3. Isodose lines of electron radiation in energies of 6, 8, 10, 12 and 15 MeV inside the polymethyl methacrylate (PMMA) phantom in a 10 × 10 cm field: A, with surgical medical mask (SMM) (under the mask); B, 5 cm next to the SMM (no mask).

Table 1. Dose Enhancement Ratio and Transmission Factor Calculated from Monaco for 6, 10, and 18 MV X-ray Exposure

Energy (MeV)	At d = 100 mm Depth (%)	
	Dose Enhancement Ratio	Transmission Factor
6	0.52	0.96
10	0.49	0.96
18	0.19	0.99

diminishes as photon energy increases. For electron beams, it was observed that the density of high-percentage isodose lines was greater in the open field than under the mask. This indicates a measurable attenuation effect caused by the SMM.

The impact of the metal strip on dose distribution changes in both photon and electron radiation is illustrated in Figures 2B and 3B, respectively. The presence of the metal strip resulted in a shift of low-energy isodose lines toward the surface of the phantom, highlighting the influence of the strip on surface dose enhancement.

4.2. Dose Measurements

4.2.1. Photon Percentage Depth Dose

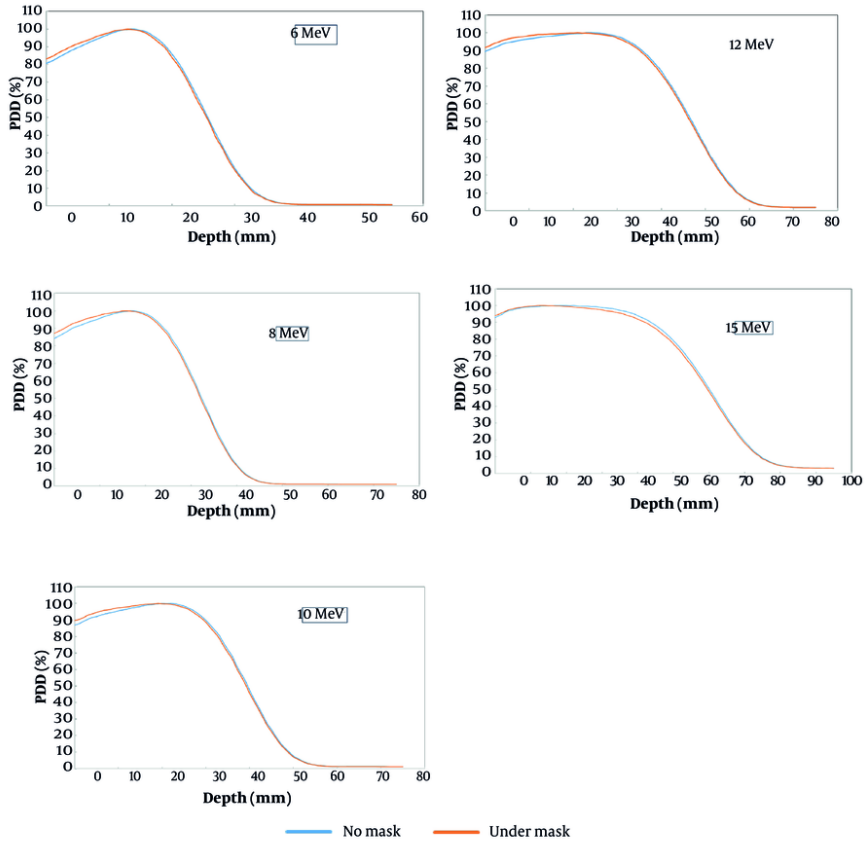

Figure 4. Percentage depth dose (PDD) curves, in open field and under surgical medical mask (SMM) for 6, 8, 10, 12 and 15 MeV electron radiation (in field PDD).

Percentage depth dose data were obtained for both in-field and out-of-field scenarios: Open field without SMM (no mask), and field with SMM (with mask) for all photon energies (6, 10, and 18 MV).

A comparison between the dose distributions measured with and without the SMM revealed significant discrepancies in the PDD curves, particularly from the surface to a depth of 20 mm. Based on the MER, the maximum increase in dose was observed at the entrance plane of the phantom. Higher doses were recorded under the SMM compared to the unmasked field. Specifically, the masked readings increased by: 1.2 times for 6 MV, 1.18 times for 10 MV, and 1.14 times for 18 MV photons. This observation suggests that the SMM behaves like a bolus, increasing the surface dose — an effect most pronounced at the lowest energy level (6 MV).

When the SMM was placed outside the field, the PDD in the unmasked state was lower than in the masked state. This increase can be attributed to scatter radiation caused by the presence of the SMM. Additionally, as photon energy increased, the difference between masked and unmasked curves decreased. Out-of-field measurements showed: For 6 MV photons, the dose at depths of 100 mm and 150 mm was 8.5% higher in the masked state compared to the unmasked state; for 10 MV photons, the dose was 6.8% and 7.1% higher at those respective depths; for 18 MV photons, the corresponding increases were 6.8% and 4.4%, respectively.

We also found that in terms of maximum PDD depth: For 6 MV, there was no change compared to the unmasked condition; for 10 MV, the depth of maximum dose shifted approximately 1 mm closer to the surface; and for 18 MV, this shift was about 2 mm. The influence

of the metal strip embedded in the mask was also evident, causing a noticeable change in dose distribution. This can be seen in the right corners of Figures 2A and 3A, where the presence of the metal component led to an increase in surface dose.

4.2.2. Electron Percentage Depth Dose

The PDD curves for 6, 8, 10, 12, and 15 MeV electron energies were plotted along the central axis of the beam, both with and without the presence of the SMM, as shown in Figure 4.

Analysis of these graphs reveals that before the depth of maximum dose, the PDD in the masked state is higher than in the unmasked state, whereas after the buildup depth, this relationship is reversed. The difference percentage was measured up to a depth of 12 mm. As the electron energy increased, the difference between the masked and unmasked PDD curves decreased. Specifically, the masked readings increased by: 3.1% for 6 MeV, 3.4% for 8 MeV, 3.2% for 10 MeV, 2.6% for 12 MeV, and 1.3% for 15 MeV, compared to the unmasked condition. This indicates an increase in surface dose, which was most pronounced for 8 MeV and least for 15 MeV. As depth increased, the dose difference between masked and unmasked conditions decreased across all energies. For higher-energy electron beams, after a certain depth, the trend reversed, with the masked dose becoming lower than the unmasked dose — leading to a negative difference percentage. These observations suggest that the presence of the SMM on the surface acts as a water-equivalent bolus, increasing the surface dose. However, at higher energies, this bolus-like effect diminishes, and beyond the depth of maximum dose, the mask contributes to a greater attenuation of energy in depth.

With the SMM in place, the depth of maximum PDD shifted toward the surface as follows: By approximately 1 mm for 6 and 8 MeV, 2 mm for 10 and 12 MeV, and about 3 mm for 15 MeV.

5. Discussion

We investigated the effect of face masks used during the COVID-19 pandemic on the radiation field. A series of dosimetric evaluations were conducted to assess the changes in dose distribution under and around the SMM when exposed to RT using various photon and electron beam energies. Both absolute and relative doses were measured within the irradiated fields and outside the fields beneath the SMM for different photon and electron energies.

The results from the dose calculations indicated that the dose distribution under the SMM differed slightly from that in the unmasked state. These differences were more noticeable in electron radiation. In electron therapy, at superficial depths within the phantom, the dose under the SMM was higher than in the unmasked field. However, this trend reversed with increasing depth, particularly beyond the point of maximum dose. Similar findings were reported by Steinman et al. and Napier et al., who studied the effects of tri-layered cloth on electron field dose distribution (13, 16). These results support the conclusion that the SMM behaves like a bolus, enhancing the superficial dose.

Few studies have focused on dose measurement under the SMM. In a study conducted by Wang et al. in 2021 (18), the presence of a mask within the treatment field of proton RT resulted in only minimal dose changes. In our study, although the observed changes were relatively small, they are not negligible and should be considered during the treatment planning process.

Regarding photon exposure to areas surrounding the SMM, a slight dose increase was observed in the adjacent regions (Figure 2A). Similar out-of-field dose effects have been reported in other studies (19), which are believed to result from scatter radiation generated by the mask material, thereby increasing the dose. This dose distribution outside the main beam is clinically relevant, particularly in the treatment of breast cancer with supraclavicular lymph node involvement, where parts of the radiation field may be either covered by the patient's medical mask or located very close to it. This proximity restricts the use of the SMM within or near the irradiated field. Nevertheless, the observed dose increase in these regions is very small and may be considered clinically negligible when weighed against the protective role of the SMM in preventing COVID-19 infection.

The effect of the metal clamp embedded in the SMM was also evaluated within the radiation field. Our calculations demonstrated that the presence of metal increases the surface dose, which may lead to cutaneous complications. These findings are consistent with other studies that have documented the impact of metallic components on altering the radiation dose distribution (17). As illustrated in Figures 2 and 3, in areas where the metal strip is located, low isodose lines are shifted toward the surface. To mitigate such dosimetric artifacts

while maintaining safety protocols, collaborative efforts between medical physicists, radiation therapists, and mask manufacturers are recommended. These efforts could lead to the standardization of mask designs that minimize radiation dose interference without compromising the essential functionality of the metal strip.

5.1. Conclusions

This study was conducted on tri-layered SMMs commonly worn by patients during the COVID-19 pandemic. The material of these masks is similar to that used in patient gowns. Notably, folds or pockets in patient clothing can create an equivalent thickness to that of the mask. For patients who decline to remove their clothing, even within the treatment area, there is potential for altered dose delivery to the targeted treatment zones.

Our findings demonstrated that a thickness of approximately 10 mm, as found in tri-layered masks, can lead to variations in dose distribution for both photon and electron radiation, affecting areas within the main treatment field as well as outside the field. Based on these results, it is strongly recommended to ensure that patients' medical masks, clothing, and diapers are kept out of the irradiated field area. Where feasible, this guidance should be extended to maintain dose accuracy and avoid unintentional alterations in treatment delivery.

Footnotes

Authors' Contribution: The conception and design of the study: A. J. E.; Acquisition of data: A. J. E., L. A., and M. R. S.; Analysis and interpretation of data: A. J. E., L. A., and M. R. S.; Drafting the article or revising it critically for important intellectual content: A. J. E.; Final approval of the version to be submitted: A. J. E., L. A., and M. R. S.

Conflict of Interests Statement: The authors declare no conflict of interest.

Data Availability: The dataset presented in the study is available on request from the corresponding author during submission or after its publication.

Ethical Approval: IR.QUMS.REC.1400.296 .

Funding/Support: This work was supported by the Research Chancellor of Qazvin University of Medical Sciences (grant no.: 400000353).

References

1. Mohindra P, Buckey CR, Chen S, Sio TT, Rong Y. Radiation therapy considerations during the COVID-19 Pandemic: Literature review and expert opinions. *J Appl Clin Med Phys*. 2020;**21**(5):6-12. [PubMed ID: 32324950]. [PubMed Central ID: PMC7286011]. https://doi.org/10.1002/acm2.12898.
2. Lancia A, Bonzano E, Bottero M, Camici M, Catellani F, Ingrosso G. Radiotherapy in the era of COVID-19. *Expert Rev Anticancer Ther*. 2020;**20**(8):625-7. [PubMed ID: 32552073]. https://doi.org/10.1080/14737140.2020.1785290.
3. Tang LV, Hu Y. Poor clinical outcomes for patients with cancer during the COVID-19 pandemic. *Lancet Oncol*. 2020;**21**(7):862-4. [PubMed ID: 32479788]. [PubMed Central ID: PMC7259901]. https://doi.org/10.1016/S1470-2045(20)30311-9.
4. Yang K, Sheng Y, Huang C, Jin Y, Xiong N, Jiang K, et al. Clinical characteristics, outcomes, and risk factors for mortality in patients with cancer and COVID-19 in Hubei, China: a multicentre, retrospective, cohort study. *Lancet Oncol*. 2020;**21**(7):904-13. [PubMed ID: 32479787]. [PubMed Central ID: PMC7259917]. https://doi.org/10.1016/S1470-2045(20)30310-7.
5. Zhang L, Zhu F, Xie L, Wang C, Wang J, Chen R, et al. Clinical characteristics of COVID-19-infected cancer patients: a retrospective case study in three hospitals within Wuhan, China. *Ann Oncol*. 2020;**31**(7):894-901. [PubMed ID: 32224151]. [PubMed Central ID: PMC7270947]. https://doi.org/10.1016/j.annonc.2020.03.296.
6. Lewis MA. Between Scylla and Charybdis - Oncologic Decision Making in the Time of Covid-19. *N Engl J Med*. 2020;**382**(24):2285-7. [PubMed ID: 32267650]. https://doi.org/10.1056/NEJMp2006588.
7. Bayersdorfer J, Giboney S, Martin R, Moore A, Bartles R. Novel manufacturing of simple masks in response to international shortages: Bacterial and particulate filtration efficiency testing. *Am J Infect Control*. 2020;**48**(12):1543-5. [PubMed ID: 32682015]. [PubMed Central ID: PMC7363600]. https://doi.org/10.1016/j.ajic.2020.07.019.
8. Wang Y, Deng Z, Shi D. How effective is a mask in preventing COVID-19 infection? *Med Devices Sens*. 2021;**4**(1). e10163. [PubMed ID: 33615150]. [PubMed Central ID: PMC7883189]. https://doi.org/10.1002/mds3.10163.
9. Kunstler B, Newton S, Hill H, Ferguson J, Hore P, Mitchell BG, et al. P2/N95 respirators & surgical masks to prevent SARS-CoV-2 infection: Effectiveness & adverse effects. *Infect Dis Health*. 2022;**27**(2):81-95. [PubMed ID: 35151628]. [PubMed Central ID: PMC8769935]. https://doi.org/10.1016/j.idh.2022.01.001.
10. Nalunkuma R, Abila DB, Ssewante N, Kiyimba B, Kigozi E, Kisuza RK, et al. Double Face Mask Use for COVID-19 Infection Prevention and Control Among Medical Students at Makerere University: A Cross-Section Survey. *Risk Manag Healthc Policy*. 2022;**15**:111-20. [PubMed ID: 35087291]. [PubMed Central ID: PMC8789312]. https://doi.org/10.2147/RMHP.S347972.
11. Burnett R, Spadaro J. Global Mortality and Long-Term Ambient Exposure to Fine Particulate Matter: A New Relative Risk Estimator. *ISEE Conference Abstracts*. 2018;**115**(38). https://doi.org/10.1289/isesisee.2018.S02.04.33.
12. Ding Y, Ma P, Li W, Wei X, Qiu X, Hu D, et al. Effect of Surgical Mask on Setup Error in Head and Neck Radiotherapy. *Technol Cancer Res Treat*. 2020;**19**:1533033820974020. [PubMed ID: 33327884]. [PubMed Central ID: PMC7750894]. https://doi.org/10.1177/1533033820974021.

13. Steinman JP, Hopkins SL, Wang IZ. Dosimetric perturbation from cloth and paper gowns for total skin electron irradiation. *J Appl Clin Med Phys*. 2013;**14**(4):4045. [PubMed ID: 23835373]. [PubMed Central ID: PMC5714533]. https://doi.org/10.1120/jacmp.v14i4.4045.

14. Oulhouq Y, Zerfaoui M, Bakari D, Rrhioua A, Machichi M, Berhili S. The comparison of two calculation algorithms to evaluate the dosimetric effects of thermoplastic masks used in radiotherapy. *Materials Today: Proceedings*. 2019;**13**:1102-7. https://doi.org/10.1016/j.matpr.2019.04.077.

15. Miura H, Hioki K, Ozawa S, Kanemoto K, Nakao M, Doi Y, et al. Uncertainty in the positioning of patients receiving treatment for brain metastases and wearing surgical mask underneath thermoplastic mask during COVID-19 crisis. *J Appl Clin Med Phys*. 2021;**22**(6):274-80. [PubMed ID: 34028970]. [PubMed Central ID: PMC8200509]. https://doi.org/10.1002/acm2.13279.

16. Napier ID, Locke J, Grubb SR, Picton DJ. Contamination skin doses and attenuation of radiation by clothing. *J Radiol Prot*. 2010;**30**(4):717-33. [PubMed ID: 21149936]. https://doi.org/10.1088/0952-4746/30/4/006.

17. Le Fevre C, Brinkert D, Menoux I, Kuntz F, Antoni D, El Bitar Z, et al. Effects of a metallic implant on radiotherapy planning treatment-experience on a human cadaver. *Chin Clin Oncol*. 2020;**9**(2):14. [PubMed ID: 32075394]. https://doi.org/10.21037/cco.2020.01.09.

18. Wang YM, Hsieh YW, Huang BS, Sung KC, Juan KJ, Lee SP, et al. Medical Mask Wearing During Treatment for Patients Undergoing Radiotherapy in COVID-19 Pandemic - An Experience of Protocol Setup and Dosimetric Evaluation for Particle/Proton Beam Therapy. *Risk Manag Healthc Policy*. 2021;**14**:869-73. [PubMed ID: 33688283]. [PubMed Central ID: PMC7936699]. https://doi.org/10.2147/RMHP.S286404.

19. Mahmoudi L, Mostafanezhad K, Zeinali A. Performance evaluation of a Monte Carlo-based treatment planning system in out-of-field dose estimation during dynamic IMRT with different dose rates. *Inform Med Unlocked*. 2022;**29**. https://doi.org/10.1016/j.imu.2022.100912.